Comparison of loading double-loop microtraps from a surface MOT and a FORT

B. Jian · W. A. van Wijngaarden

Abstract Two methods to load a microtrap consisting of two concentric microwire loops of radii 300 and 660 μm carrying oppositely oriented currents are demonstrated. Atoms can be directly loaded into the microtrap from a surface magneto-optical trap or alternatively using a far-off resonance optical dipole trap (FORT) as an intermediate step. About 1×10^5 ^{87}Rb atoms can be loaded into the microtrap using either technique although the FORT achieves a lower temperature. The FORT is well suited to loading a linear array of 3 microtraps that are aligned with the propagation direction of the infrared laser. Atoms can be trapped in either the $5S_{1/2}$ $F = 1$ or 2 ground state hyperfine level. The position of the microtrapped atom cloud can be precisely adjusted using a bias magnetic field over a distance of 350 to slightly <50 μm from the atom chip surface.

1 Introduction

Magnetic microtraps containing ultracold neutral atoms [1–4] are facilitating a growing number of applications such as surface studies [5], Michelson interferometers on an atom chip [6], atom-field coupling for a Bose Einstein condensate in an optical cavity [7] and quantum information processing [8]. Recently, our group demonstrated a microtrap consisting of two concentric circular microwire loops that generates a 3-D trap [9]. This microtrap does not require fields generated by macroscopic coils unlike the conventional U- and Z-traps [10]. Moreover, it can be

B. Jian · W. A. van Wijngaarden (✉)
Physics Department, York University, Petrie Building,
4700 Keele Street, Toronto, ON M3J 1P3, Canada
e-mail: wlaser@yorku.ca

linked in series to create a linear array of microtraps. Atoms loaded into the microtrap were first prepared in a conventional magneto-optical trap (MOT) and then transported to the atom chip using magnetic fields.

The challenge to load a microtrap is that its trap volume is orders of magnitude smaller than for a MOT. This work shows two relatively simple methods to load ^{87}Rb atoms into the microtrap using a surface MOT and a far-off resonance trap (FORT). A comparable number of atoms were loaded into the microtrap array as in the earlier work but at a temperature over an order of magnitude lower [9]. This facilitates precisely positioning the microtrapped atom cloud using a bias field to within 50 μm of the atom chip surface. The paper is organized as follows. First, the microtrap and the associated apparatus are described. Next, the experimental procedure is presented, and detailed results of the two loading schemes are given. Finally, conclusions are made.

2 Apparatus

The linear array of double-loop microtraps is illustrated in Fig. 1. It was fabricated by lithographically depositing a 10-μm-thick copper layer onto a silicon wafer. Each of the three microtraps, separated by 1.5 mm, was formed by the magnetic field generated by the currents I flowing through two concentric loops in opposite directions. The radii of the inner and outer loops were $r_1 = 300$ μm and $r_2 = 660$ μm, respectively, and the microwire width was 50 μm. The ratio $r_2/r_1 = 2.2$, which maximized the force an atom experiences along the z axis as has been explained previously [9].

Figure 1 shows that the magnetic field has a minimum along the x, y and z axes to produce a 3-D trap. The trap
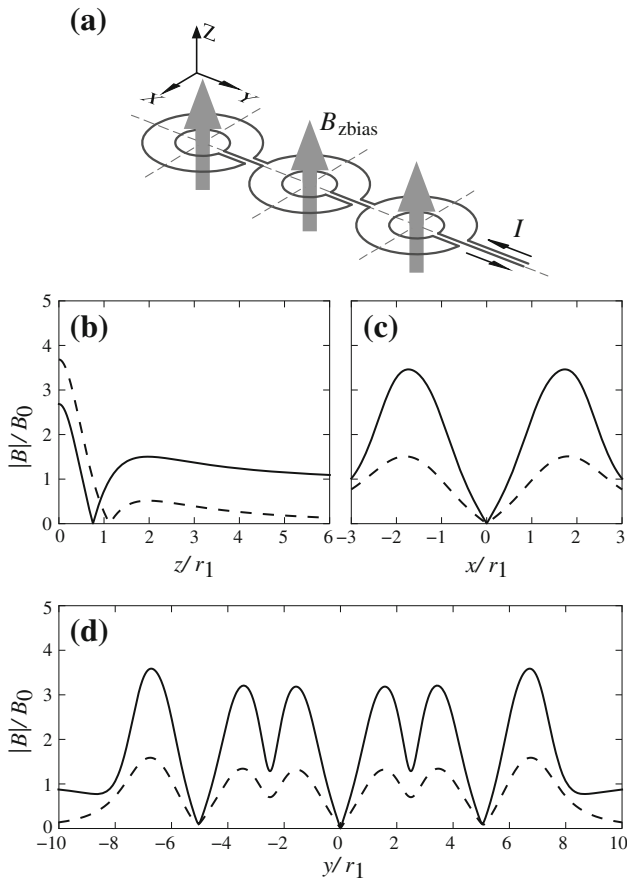
Fig. 1 Microtrap array configuration. Each of the three microtraps shown in **a** consists of two concentric microwire loops of radii r_1 and $r_2 = 2.2r_1$. The trap centers are located at a distance $5r_1$ apart. The dependence of the magnetic field magnitude along the z, x and y directions as measured from the center of the middle microtrap is shown in **b–d** for the case of zero bias field (*dashed line*) and $B_{zbias} = B_o$ (*solid line*)

depth increased by applying a bias field in the z direction, B_{zbias}. Figure 1 considers the case $B_{zbias} = B_o$ where $B_o = \frac{\mu_o}{4\pi} \frac{I}{r_1}$ and μ_o is the permeability of vacuum. The bias field also shifts the trap position along the z direction closer to the atom chip surface. In our experiment, a typical chip current of 2.6 A corresponding to $B_o = 8.67$ G generated a trap depth of 300 μK for ^{87}Rb atoms occupying the $|F = 2, m_F = 2\rangle$ sublevel where m_F denotes the Zeeman quantum number of the ground state hyperfine level F. The trap depth increased to 870 μK when a bias field equal to B_o was applied.

The apparatus is illustrated in Fig. 2. Thermally conductive epoxy (EpoTek H77) was used to attach the atom chip to a copper block, which was in turn supported by a vacuum flange. The copper block was encapsulated by a borosilicate glass cell. The vacuum system was pumped down using a turbo molecular pump and a combination of ion/titanium sublimation pump to a pressure of 7×10^{-10}
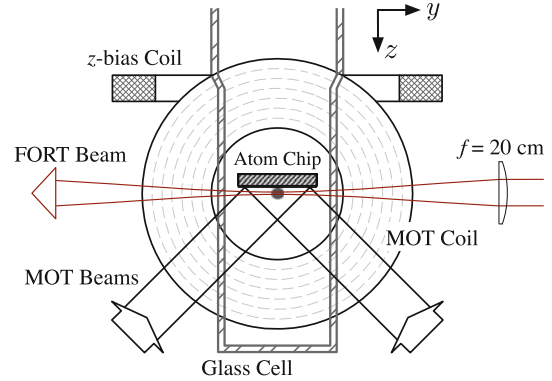

Fig. 2 Apparatus. The surface MOT denoted by a *black dot* below the chip surface was generated at the intersection of the 45° MOT laser beams, consisting of overlapping trapping and repump laser beams as is described in the text, with two laser beams counter propagating in the direction perpendicular to the page which are not shown

torr. The glass cell was surrounded by a pair of coils that generated the quadrupole field for the surface MOT. The MOT coils were aligned along the x direction, parallel to the atom chip surface in contrast to the traditional 45° arrangement [11]. This simplified the apparatus. The MOT laser beams were directed along the $\pm x$ directions as well as in the radial direction of the quadrupole field and reflected off the atom chip surface.

Two pairs of coils, centered about a point 2 mm below the atom chip surface, generated bias fields along the x and y directions, which positioned the MOT exactly below the microtrap array. A single square coil (11 × 11 cm^2) consisting of 72 turns and located 3.9 cm above the atom chip generated the B_{zbias} field which at the microtrap array was 4.2 G/A predominantly in the vertical z direction. B_{zbias} not only affected the microtrap operation as discussed previously but was also used to shift the MOT atom cloud toward the atom chip surface to facilitate loading the microtraps.

Standard laser cooling techniques were utilized as are described elsewhere [12]. A trap laser was red detuned from the $5S_{1/2} F = 2 \rightarrow 5P_{3/2} F' = 3$ transition while a repump laser was frequency locked to the $5S_{1/2} F = 1 \rightarrow 5P_{3/2} F' = 2$ transition. Ultracold atom clouds were probed using the absorption imaging method [13, 14]. The probe laser beam was circularly polarized and resonant with the $5S_{1/2} F = 2 \rightarrow 5P_{3/2} F' = 3$ transition. The probe beam propagation direction made a small ($\leq 5°$) angle with respect to the x axis to avoid interfering with two of the MOT laser beams. The probe laser spatial profile had a radius of about 0.6 cm and was partially blocked by the atom chip. The probe beam passed through the atom cloud and was observed using a 1:1 imaging lens system and a CCD camera. A typical probe laser pulse had a power of

100 µW and a duration of 50 µs. Atoms in the $F = 1$ ground state hyperfine level could be detected by temporally and spatially overlapping the repump and probe laser beams.

3 Loading a microtrap from a surface MOT

The procedure to load the microtrap is given in Table 1. Atoms were first collected into a surface MOT from the background rubidium vapor [10, 11]. Figure 2 displays one of the quadrupole coils used to generate the surface MOT. A typical magnetic field gradient of 14 G cm^{-1} was used. This figure also shows one pair of MOT laser beams that reflected off the copper chip surface. The trap laser had an intensity of 47 mW/cm^2 and a detuning of 14 MHz while the repump laser intensity was 2.4 mW/cm^2. Approximately 3×10^7 atoms were loaded into the surface MOT in 6 s. The MOT cloud had a diameter of 1.5 mm and was positioned 2 mm below the atom chip surface.

The MOT cloud was compressed (CMOT) by increasing the field gradient to 35 G cm^{-1} during a time of 50 ms. During the CMOT stage, the trap laser detuning was increased to 30 MHz and the repump laser intensity was reduced to 0.2 mW/cm^2. Small bias fields were applied in the x, y and z directions to position the MOT cloud directly beneath the middle microtrap. The alignment of the MOT with the microtrap array was checked by observing the imaging laser beam reflected off the atom chip surface. The CMOT cloud consisted of 1.1×10^7 atoms and was positioned 0.5 mm below the atom chip.

The next stage was to cool the atoms using optical molasses for 8 ms. All magnetic fields were switched off, and the trap laser detuning was increased to 50 MHz. The atom temperature was measured using the time of flight method to be 35 µK. The atoms were optically pumped to the $|2, 2\rangle$ magnetically trapped Zeeman sublevel using a 1 ms circularly polarized laser beam resonant with the $5S_{1/2}\ F = 2 \rightarrow 5P_{3/2}\ F' = 2$ transition. The 100 µW optical pumping laser beam overlapped with a small fraction of the repump laser beam power and was directed in the $-x$ direction. A x-bias field of 3 G defined the quantization axis.

Atoms were transferred into the microtrap by suddenly blocking all laser beams and turning on the chip and z-bias currents. The probe laser imaged the microtrap for times between 30 and 600 ms after atoms were loaded into it. The minimum time of 30 ms allowed atoms not loaded into the microtrap to disperse to obtain a clear image of the microtrapped atom cloud. The number of trapped atoms was unlikely to be reduced significantly during this initial 30 ms due to plain evaporative cooling since the trap depth is about an order of magnitude greater than $k_B T$ where k_B is Boltzmann's constant and T is the atom temperature [15].

Figure 3a shows an example of microtrapped atoms obtained using a z-bias coil current of 0.7 A. The maximum number of trapped atoms, found by varying the chip current up to 5 A, occurred at 2.6 A. Only the middle microtrap was loaded because the CMOT atom cloud did not spatially extend to the left and right microtraps. Figure 3b shows that the optical density of the microtrapped cloud profile was fitted well by a Gaussian function having a radius (HWHM width) of 100 µm. A maximum of 1.6×10^5 atoms could be loaded into the microtrap corresponding to a peak density of 5.2×10^9 cm^{-3}. The atom temperature of 107 µK was estimated by measuring the cloud radius as a function of the probe delay time of up to 2 ms after the microtrap was turned off. This is higher than after the optical molasses stage, which may be due to heating caused by optical pumping. Another possibility is that atoms gained potential energy when the microtrap was suddenly switched on, which was subsequently converted to kinetic energy.

Figure 4a shows the dependence of the number of microtrapped atoms as a function of the z-bias field current. A significant number of atoms could be loaded into the microtrap without using any z-bias field. The atom number obtained by optically pumping the atoms into the $|2, 2\rangle$

Table 1 Typical timing sequence of loading microtrap using a surface MOT and a FORT

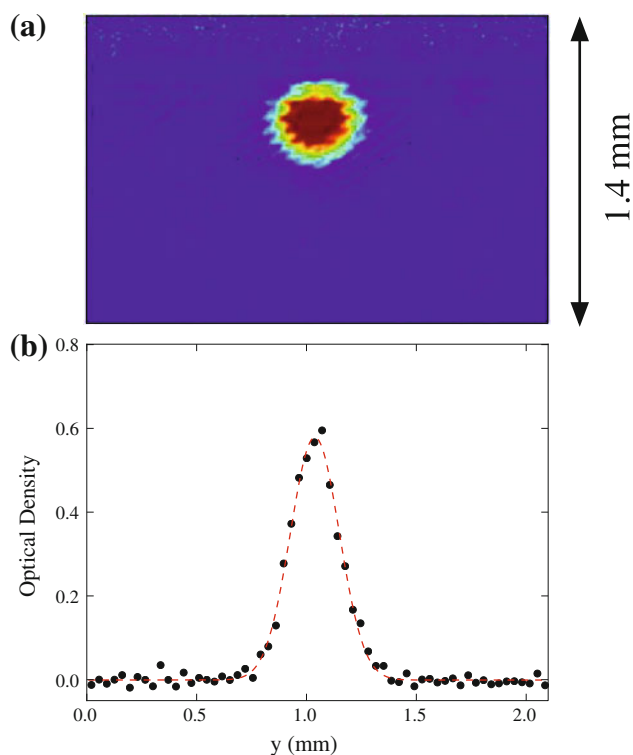| Surface MOT loading	Interval	FORT loading	Interval
MOT loading	6 s	MOT loading	6 s
CMOT	50 ms	CMOT + FORT loading	140 ms
Optical molasses	8 ms	FORT + optical molasses	20 ms
Optical pumping	1 ms	FORT on	40 ms
Microtrap holding	30–600 ms	Microtrap ramp on + FORT	20 ms
Probing	50 µs	Microtrap holding + FORT ramp down	40 ms
		Microtrap holding	30–600 ms
		Probing	50 µs

Fig. 3 **a** Absorption image of atoms trapped in the middle microtrap loaded from a surface MOT for a $B_{z\text{bias}}$ current of 0.7 A and a chip current of 2.6 A. This image was taken 40 ms after the microtrap was turned on. The optical density is *plotted* in **b** along the *horizontal* direction through the atom cloud center. Each *point* is averaged over 5 pixels. The *red dashed line* is a Gaussian fit to the data

Fig. 4 **a** Dependence of the number of atoms in the middle microtrap loaded from a surface MOT versus the $B_{z\text{bias}}$ current for the case with (*solid dots*) and without (*open squares*) optical pumping. The microtrap position shown in **b** was nearly indistinguishable for the two cases

trapping level was significantly higher as expected. A reduction of the trapped atom number occurred at a bias current of about 1.7 A. There was no similar decrease in the absence of optically pumping. It therefore is reasonable to conclude that some atoms were lost due to Majorana spin flips to untrapped Zeeman sublevels when the microtrap center, where the magnetic field vanishes, coincided with the surface MOT. Figure 4b shows that the z-bias current shifted the center of the microtrap position relative to the atom chip. The z-bias field at which the reduction in trapped atom number occurred varied somewhat from day to day. This is believed to be caused by small changes of the MOT position, which was affected by the daily alignment of the MOT laser beams.

4 Loading microtrap array from a FORT

A FORT was generated using an infrared laser operating at 1,064 nm. The laser beam passed through an acousto-optic modulator that acted as a fast shutter and allowed adjustment of the laser power from 0 to a maximum of 14 W. The FORT was created by focusing the infrared laser beam
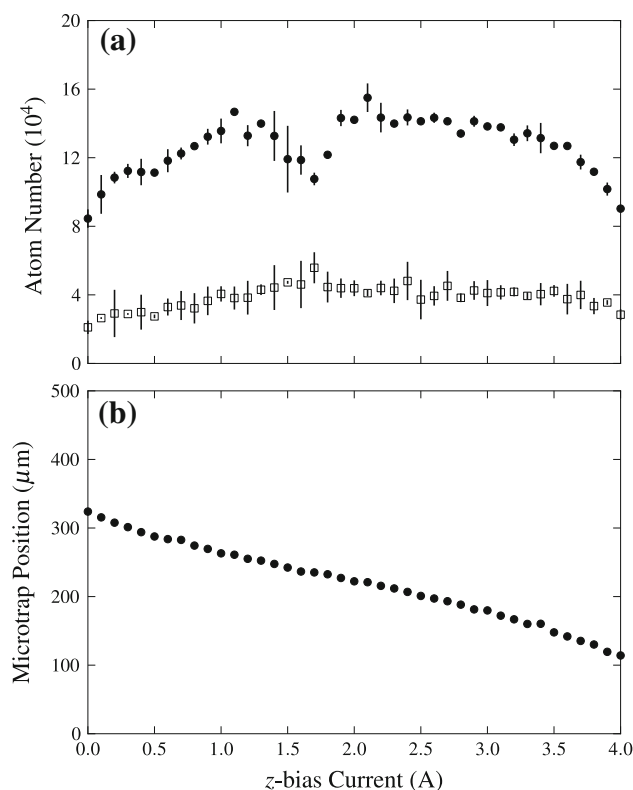
using a 20 cm focal length plano-convex lens. The radius of the focal spot was measured to be 35 µm, and the Raleigh length equaled 2.8 mm resulting in a trap depth of 1 mK. The FORT laser beam was aligned to overlap with the surface MOT and the microtrap array in the x and y directions. The distance between the FORT laser focus and the atom chip surface was carefully adjusted.

Table 1 describes the procedure to transfer atoms from the FORT into the microtrap array. After the surface MOT loading phase, the FORT laser was turned on and the MOT was compressed in a time of 140 ms. The parameters for the CMOT were the same as when the microtrap was loaded directly from the surface MOT. A lower repump intensity of 27 µW cm^{-2} was used to minimize heating caused by effects such as ground state hyperfine changing collisions [16].

Atoms were cooled for 20 ms during an optical molasses phase as described in Sect. 3 while the FORT laser remained on. Figure 5a shows a typical FORT cloud containing 8.5×10^5 atoms in the $F = 1$ ground state hyperfine level corresponding to a peak density of 1.3×10^{10} cm^{-3}. The atom temperature of 330 µK was found by switching the FORT laser off and observing the cloud
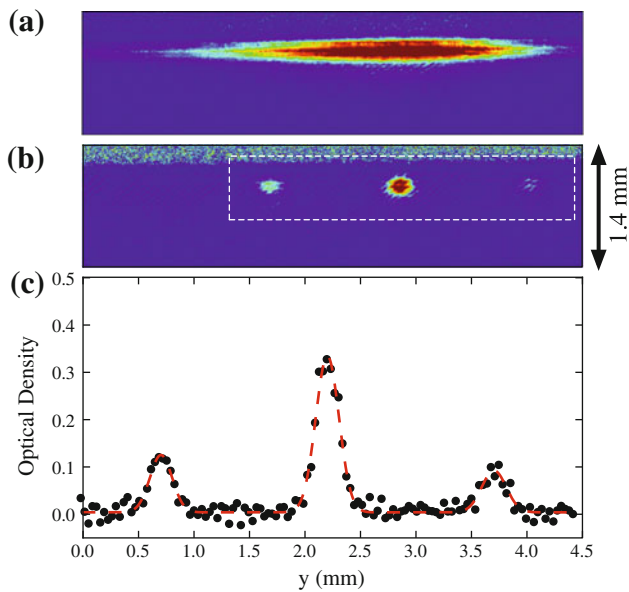
(a)

(b)

1.4 mm

(c)

Fig. 5 Absorption image of atoms trapped in **a** a FORT located about 220 μm below the atom chip surface and **b** the microtrap array for a $B_{z\text{bias}}$ current of 0.7 A showing populations of 3.4×10^4, 6.8×10^4 and 2.2×10^4 atoms in the *left*, *middle* and *right* microtraps, respectively. These two images have the same dimensions and *color scale*. This image was taken 40 ms after the microtrap was turned on. The optical density along the *horizontal* direction through the center of the middle microtrapped atom cloud is shown in **c** for the range indicated by the *white dashed box* in **b**. Each point is averaged over 5 pixels. The *red dashed line* is the sum of three Gaussian functions fitted to the data. The FORT was aligned to maximize the number of atoms loaded into the middle microtrap

expansion in the radial direction. A similar number of atoms could be prepared in the $F = 2$ ground state hyperfine level by turning off the repump laser 1 ms after the trap laser. Over 98 % of the atoms were found to occupy the same hyperfine level.

Atoms were loaded into the atom chip by linearly ramping up the chip current to 2.6 A along with the z-bias field current in 20 ms. This was followed by a linear decrease of the FORT laser power. Figure 5b shows a typical image of the microtrapped atom clouds loaded using a FORT ramp down time of 40 ms. Figure 5c shows a middle microtrap having 6.8×10^4 (4.7×10^4) atoms corresponding to a density of 6.0×10^9 cm^{-3} (3.8×10^9 cm^{-3}) for atoms in the $F = 1$ ($F = 2$) ground state hyperfine level. The number of atoms loaded into the central microtrap was about half that loaded using the surface MOT. However, the sum of the populations in the three microtraps was comparable using the two loading methods. Figure 6 shows the dependence of the number of atoms in the $F = 1$ ground state hyperfine level in the middle microtrap as a function of the FORT ramp down time. The number of trapped atoms increased sharply as the ramp down duration was increased to 50 ms. There was no
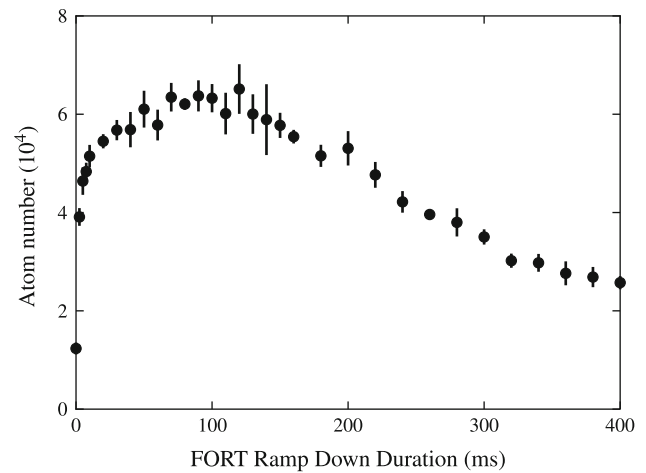

Fig. 6 Dependence of number of atoms in the middle microtrap on FORT ramp down duration
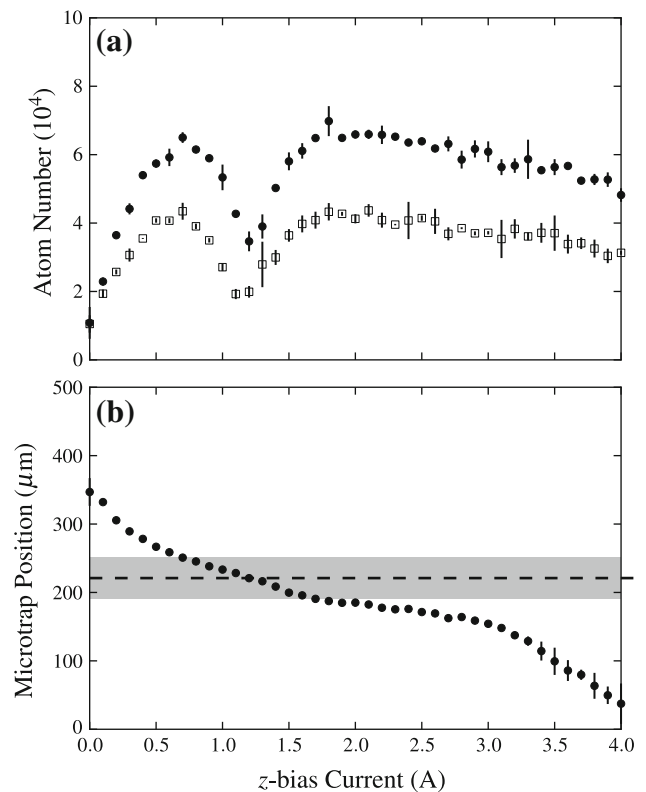
(a)

(b)

Fig. 7 **a** Dependence of the number of atoms in the middle microtrap loaded from a FORT versus the $B_{z\text{bias}}$ current for the case of atoms in the $F = 1$ (*solid dots*) and $F = 2$ (*open squares*) ground state hyperfine levels. The microtrap position shown in **b** was nearly indistinguishable for the two cases. The *dashed line* shows the position of the maximum FORT laser beam intensity, while the *gray region* indicates the region where the laser intensity exceeds half of its maximum intensity

significant change for ramp down durations between 50 and 150 ms. Thereafter, the number of trapped atoms decreased slowly.

The effect of the z-bias field on the number of atoms in the middle microtrap and its position below the atom chip surface is described in Fig. 7a. Relatively, few atoms were loaded into the microtrap at a zero $B_{z\text{-bias}}$ current. As the z-bias field increased, the microtrap position shifted closer to the FORT and the number of microtrapped atoms increased. However, at a $B_{z\text{-bias}}$ current of 1.2 A, where the microtrap position overlapped the FORT, the number of microtrapped atoms was reduced significantly. Several different FORT positions ranging from 187 to 350 μm below the atom chip surface were investigated, and a reduction in the number of microtrapped atoms occurred whenever the centers of the microtrap and FORT overlapped. This phenomenon can be explained by Majorana spin flips of the atoms occurring near the microtrap center. Trap loss was therefore maximized when the microtrap and FORT trap centers coincided. The atom loss shown in Fig. 7a is significantly larger than that shown in Fig. 4a. The FORT radius is over an order of magnitude smaller than the size of the CMOT atom cloud. Hence, atoms spend more time near the microtrap center increasing the rate of Majorana spin flips, resulting in the observed loss of trapped atoms [17].

Figure 7a shows that more atoms in the $F = 1$ ground state hyperfine level were loaded into the microtrap than in the $F = 2$ level. This difference occurred because the two hyperfine levels have different numbers of Zeeman sublevels, not all of which are magnetically trapped. Figure 7b shows the microtrapped atom cloud approached the atom chip surface as the z-bias magnetic field increased. The temperature of the microtrapped atoms was measured to be 30 and 47 μK for atoms in the $F = 1$ and 2 hyperfine levels, respectively. These temperatures were much smaller than that of atoms in the FORT as well as the temperature of the microtrapped atom cloud loaded directly from the surface MOT. The temperature reduction arises because of forced evaporative cooling facilitated by ramping down the FORT laser power [18, 19]. This temperature decrease was found to be independent of the FORT laser ramping down times of between 30 and 400 ms.

The lifetime of the microtrapped atom cloud was found by fitting the atom number versus the trap holding time with an exponential decay function. A lifetime of 350 ± 15 ms was found for atom clouds in either the $F = 1$ or 2 levels. This lifetime was consistent with that measured for the microtrap loaded from the surface MOT. Atoms are lost from the microtrap due to collisions with background gas atoms and molecules [20] as well as by Majorana spin flips [17].

5 Conclusions

This work demonstrated two relatively simple methods to load a double-loop microtrap with neutral ^{87}Rb cold atoms.

Approximately 10^5 atoms could be loaded in either the $F = 1$ or 2 ground state hyperfine levels. The microtrapped cloud had a density of about 6×10^9 cm^{-3} and experienced a lifetime of several hundred ms. The number of atoms loaded depended strongly on either the surface MOT or FORT cloud being in close proximity to the microtrap. However, exact overlap with the microtrap decreased the number of atoms loaded by as much as 50 %. This decrease occurs because there is no magnetic field at the microtrap center resulting in loss of atoms from the trap due to Majorana spin flips. A variety of traps have been created to suppress this loss such as the time-averaged orbiting potential trap (TOP) [17] and QUIC traps [21]. It has been proposed to add two straight microwires located on either side of our microtrap array to generate a nonzero magnetic field at the trap centers [22].

The advantage of a FORT is that it is easier to load an array of microtraps aligned along the FORT laser propagation direction. The populations of the three microtraps were not equal since the Raleigh length of the FORT focus was comparable to the distance separating the microtraps. Similar microtrap populations would be expected if the microtraps were more closely spaced. The atoms loaded using the FORT also had significantly lower temperature than occurred when the microtrap was loaded directly from the surface MOT. The microtrap position above the atom chip depends on the radius of the inner microloop and a bias field that enables the trap position to be precisely adjusted to within 50 μm of the surface. A smaller microtrap size would allow precise and convenient positioning of ultracold atoms even closer to the chip, which is of interest for studying surfaces. A 1- or 2-D array of such microtraps would allow examination of spatially varying effects.

References

1. J.D. Weinstein, K.G. Libbrecht, Phys. Rev. A **52**, 4004 (1995)
2. R. Folman, P. Krager, J. Schmiedmayer, J. Denschlag, C. Henkel, Adv. At. Mol. Opt. Phys. **48**, 263 (2002)
3. J. Fortágh, C. Zimmermann, Rev. Mod. Phys. **79**, 235 (2007)
4. D. Cano, H. Hattermann, B. Kasch, C. Zimmermann, R. Kleiner, D. Koelle, J. Fortágh, Eur. Phys. J. D **63**, 17 (2011)
5. M. Gierling, P. Schneeweiss, G. Visanescu, P. Federsel, M. Haffner, D.P. Kern, T.E. Judd, A. Gunther, J. Fortagh, Nat. Nano. **6**, 446 (2011)
6. Y.-J. Wang, D.Z. Anderson, V.M. Bright, E.A. Cornell, Q. Diot, T. Kishimoto, M. Prentiss, R.A. Saravanan, S.R. Segal, S. Wu, Phys. Rev. Lett. **94**, 090405 (2005)
7. Y. Colombe, T. Steinmetz, G. Dubois, F. Linke, D. Hunger, J. Reichel, Nature **450**, 272 (2007)
8. P. Treutlein, P. Hommelhoff, T. Steinmetz, T.W. Hänsch, J. Reichel, Phys. Rev. Lett. **92**, 203005 (2004)

9. B. Jian, W.A. van Wijngaarden, J. Opt. Soc. Am. B **30**, 238 (2013)
10. J. Reichel, Appl. Phys. B **74**, 469 (2002)
11. J. Reichel, W. Hänsel, T.W. Hänsch, Phys. Rev. Lett. **83**, 3398 (1999)
12. B. Lu, W.A. van Wijngaarden, Can. J. Phys. **82**, 81 (2004)
13. D.A. Smith, S. Aigner, S. Hofferberth, M. Gring, M. Andersson, S. Wildermuth, P. Krüger, S. Schneider, T. Schumm, J. Schmiedmayer, Opt. Express **19**, 8471 (2011)
14. C.F. Ockeloen, A.F. Tauschinsky, R.J.C. Spreeuw, S. Whitlock, Phys. Rev. A **82**, 061606 (2010)
15. K.M. O'Hara, M.E. Gehm, S.R. Granade, J.E. Thomas, Phys. Rev. A **64**, 051403 (2001)
16. S.J.M. Kuppens, K.L. Corwin, K.W. Miller, T.E. Chupp, C.E. Wieman, Phys. Rev. A **62**, 013406 (2000)
17. W. Petrich, M.H. Anderson, J.R. Ensher, E.A. Cornell, Phys. Rev. Lett. **74**, 3352 (1995)
18. C.S. Adams, H.J. Lee, N. Davidson, M. Kasevich, S. Chu, Phys. Rev. Lett. **74**, 3577 (1995)
19. M.D. Barrett, J.A. Sauer, M.S. Chapman, Phys. Rev. Lett. **87**, 010404 (2001)
20. J. van Dongen, Z. Hu, D. Clement, G. Dufour, J.L. Booth, K.W. Madison, Phys. Rev. A **84**, 022708 (2011)
21. T. Esslinger, I. Bloch, T.W. Hänsch, Phys. Rev. A **58**, R2664 (1998)
22. W.A. van Wijngaarden, Can. J. Phys. **83**, 671 (2005)